Carbohydrate Polymers 94 (2013) 394–399

Contents lists available at SciVerse ScienceDirect

Carbohydrate Polymers

journal homepage: www.elsevier.com/locate/carbpol

Amphiphilic *N*-(2,3-dihydroxypropyl)–chitosan–cholic acid micelles for paclitaxel delivery

Zheng Pan[a,*], Yunling Gao[a], Linseng Heng[a], Yi Liu[a], Gan Yao[a], Yun Wang[a], Yuping Liu[b]

[a] College of Bioinformation, Chongqing University of Posts and Telecommunication, Chongqing, China
[b] College of Chemistry and Chemical Engineering, Chongqing University, Chongqing, China

ARTICLE INFO

Article history:
Received 6 December 2012
Received in revised form 4 January 2013
Accepted 8 January 2013
Available online 16 January 2013

Keywords:
N-(2,3-Dihydroxypropyl)–chitosan–cholic acid
Micelles
Paclitaxel
Drug delivery
Antitumor

ABSTRACT

Self-assembled amphiphilic *N*-(2,3-dihydroxypropyl)–chitosan–cholic acid (DHP–CS–CHO) micelle was prepared as a carrier for paclitaxel. DHP–CS–CHO was synthesized by grafted small molecules cholic acid and glycidol onto primary amine group of chitosan, respectively. The DHP–CS–CHO formed uniform micelles (size = 212.4 ± 3.1 nm) with a low critical micelle concentration (0.024 mg/ml) in PBS. Hydrophobic anticancer drug, paclitaxel (PTX), was easily encapsulated into chitosan derivative micelles by a dialysis method with loading efficiency up to 80%. The PTX loaded micelles released the drug in a sustained manner more than a week in PBS containing 0.1% (w/v) Tween 80 at 37 °C. In vitro antitumor experiment demonstrated that PTX loaded chitosan derivative micelles could inhibit MCF-7 cell growth and induce its apoptosis. These results suggested that DHP–CS–CHO may be a promising carrier for the anticancer drug PTX.

1. Introduction

Chitosan, the *N*-deacetylated derivative of chitin, is the only one natural cationic polysaccharide composed of D-glucosamine units and *N*-acetyl-D-glucosamine units (Kim et al., 2007; Kumar, Muzzarelli, Muzzarelli, Sashiwa, & Domb, 2004). For its biocompatible, non-toxic and biodegradable characteristics, chitosan and its derivatives have received much attention in biomedical materials, such as tissue engineering and scaffolds (Muzzarelli, 2009; Muzzarelli, Boudrant, et al., 2012; Muzzarelli, Greco, Busilacchi, Sollazzo, & Gigante, 2012), drug delivery system (Chiu et al., 2009; Huang et al., 2011; Li, Wang, Peng, She, & Kong, 2011; Park, Saravanakumar, Kim, & Kwon, 2010; Trapani, Sitterberg, Bakowsky, & Kissel, 2009; Yao, Zhang, Ping, & Yu, 2007; Zheng et al., 2011). Chitosan is soluble in acidic aqueous solution, but cannot form micelles in biological or neutral solution. Therefore, different amphiphilic chitosan derivatives with good solubility in neutral solution, such as, *N*-lauryl–carboxymethyl–chitosan (Miwa et al., 1998), *N*-octyl–O-sulfate chitosan (Zhang, Ping, Zhang, & Jian, 2003; Zhang et al., 2008), cholesterol–modified glycol chitosan (Yu, Li, Qiu, & Jin, 2008), cholic acid–chitosan–g-mPEG (Ngawhirunpat et al., 2009), mPEG-g–chitosan (Liang et al., 2011), 3-diethylaminopropyl–bearing glycol chitosan (Oh et al., 2010), glycol chitosan–cholanic acid (Hwang, Kim, Kwon, & Kim, 2008; Min et al., 2008; Nam et al., 2010), glycol chitosan–deoxycholic acid (Kim et al., 2005), palmitoyl glycol chitosan (Wang, McConaghy, Tetley, & Uchegbu, 2001), cholesterol–modified O-carboxymethyl chitosan (Wang, Liu, Weng, & Zhang, 2007), deoxycholic acid modified carboxymethyl chitosan (Jin et al., 2012), deoxycholic acid–O-carboxmymethylated chitosan–folic acid (Wang et al., 2011, 2012), and so on, have been synthesized so as to deliver different drugs.

In this study, we utilized a simple chemical modification of chitosan based on the primary amine in D-glucosamine units reacted with carboxyl of hydrophobic molecule cholic acid under the catalysis of EDC and with glycidol under the catalysis of hydrogen ion, respectively, to get a new amphiphilic chitosan derivative, DHP–CS–CHO and prepared its micelles based on self-assembly. Furthermore, paclitaxel (PTX), an anticancer drug which has been used in clinical treatment of several solid tumor such as ovarian cancer, breast cancer and lung cancer, was loaded in DHP–CS–CHO micelles by dialysis. Both the PTX release profile from the PTX loaded micelles and the antitumor efficiency of the PTX loaded micelles in vitro were investigated.

2. Experimental

2.1. Materials

Chitosan (M_W = 20 kDa) was provided by the Zhejiang goldenshell biochemical Co. Ltd. (China) with deacetylation degrees of 97%. PTX was obtained by Yunnan HanDe biotechnology

* Corresponding author. Tel.: +86 023 62461884; fax: +86 023 89029056.
E-mail address: letter2012@yahoo.cn (Z. Pan).

0144-8617/$ – see front matter.
http://dx.doi.org/10.1016/j.carbpol.2013.01.013

Co. Ltd. (China). 1-Ethyl-3-(3-dimethylaminopropyl) carbodimide hydrochloride (EDC·HCl) was purchased from Y-Y (Shanghai) chemical reagent Co. Ltd. (China). Cholic acid, glycidol, 3-[4,5-dimethylthiazoly-2]-2,5-diphenyl tetrazolium bromide (MTT), pyrene and methanol (HPLC grade) were purchased from Acros Organics. All other chemicals were of analytical grade and were used without further purification.

2.2. Synthesis of DHP–CS–CHO

The modified chitosan was prepared as follow. First, chitosan (2.000 g) was dissolved in 100 ml water with the pH at 5. Then the mixture cholic acid (1.464 g) and EDC (0.824 g) in 50 ml methanol solution was added dropwise into chitosan solution. The reaction was allowed to proceed at room temperature for 24 h. After that, the reaction mixture was poured into 200 ml methanol and the pH of mixture solution was adjusted above 7 with NaOH (2 M) solution. The precipitate was filtered and washed with methanol, water and ethanol respectively more than three times until unreacted cholic acid and other impurities were removed. Then, the product chitosan–cholic acid was dried under vacuum at 40 °C. Chitosan–cholic acid (1.0 g) was suspended in 50 ml distilled water with 1% (v/v) acetic acid and stirred overnight. Then, 1.6 g glycidol was dropped into chitosan–cholic acid suspension. The reaction mixture was stirred for 24 h at 50 °C prior to termination upon the addition of NaOH (2 M) until the pH of solution above 7. Finally, the filtered solution was dialyzed against distilled water and lyophilized to yield a final product, DHP–CS–CHO (Fig. 1).

The chemical structure of DHP–CS–CHO and the degree of substitution of hydrophobic molecular cholic acid and hydrophilic molecular glycidol were characterized by FTIR (MagnaIR550II, Nicolet, USA), elemental analysis (CE440, Exter Analytical, USA) and NMR spectroscopy (Avance500, Bruker, Switzerland).

2.3. Preparation of DHP–CS–CHO micelles

DHP–CS–CHO self-assembled micelles were prepared by sonication. Briefly, DHP–CS–CHO was dissolved in PBS (pH 7.4) at the concentration of 1 mg/ml. Then, the solution was sonicated with a probe sonicator at 40 W for 2 min. To prevent the temperature of sample solution increased, the pulse of sonication was turn on 2 s with interval of 2 s. The sample solution was then filtered with 0.45 μm syringe filter.

2.4. Critical micelle concentration (CMC)

The critical micelle concentration (CMC) of DHP–CS–CHO in PBS was estimated by fluorescence spectroscopy using pyrene as hydrophobic fluorescence probe. The pyrene solutions (6.0×10^{-5} M) in methanol were added into the test tubes and evaporated under a stream of nitrogen gas to remove the methanol. A serial of DHP–CS–CHO solutions with different concentrations ranging from 1×10^{-4} to 1 mg/ml were prepared and then left to equilibrate with a constant pyrene concentration of 6.0×10^{-7} M for 24 h at 37 °C. Fluorescence spectra of pyrene were recorded with a RF5301PC spectrofluorophotometer (Shimadzu, Japan) at room temperature. The emission spectra were recorded from 350 to 450 nm at the excitation wavelength of 337 nm. Both excitation and emission brandwidths were 2.5 nm. The peak height intensity ratio (I_1/I_3) of the first peak (I_1 at 373 nm) to the third peak (I_3 at 383 nm) was plotted against the logarithm of polymer concentration. The intersection of the tangent to the curve at the inflection with the horizontal tangent through the points at low polymer concentrations was taken as the CMC value (Kalyanasundaram & Thomas, 1977).

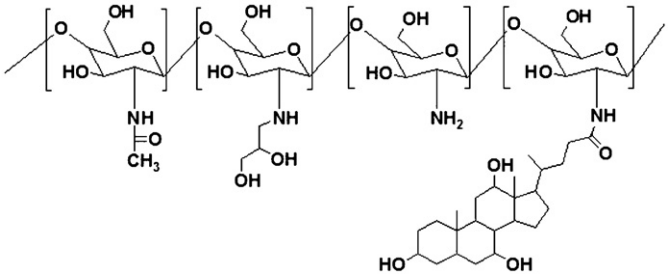

Fig. 1. Chemical structure of DHP–CS–CHO.

2.5. Size and morphology of DHP–CS–CHO micelles

The sizes of DHP–CS–CHO micelles (1 mg/ml) and PTX-loaded micelles were measured by dynamic light scattering using a Zetasizer Nano ZS90 (Malvern Instruments, Malvern, U.K.). The sample measurement was repeated 5 times and an average value was obtained. The morphologies of DHP–CS–CHO micelles and PTX-loaded micelles were analyzed by TEM (FEI Tecnai20). Briefly, prepared sample solution was dropped onto the carbon-coated 300 mesh copper grids. Then, the grids were air dried at room temperature and imaged with an electron kinetic energy of 200 keV.

2.6. Drug loading and in vitro release

PTX was loaded into the cores of the DHP–CS–CHO micelles via membrane dialysis. Briefly, 20 mg of DHP–CS–CHO was mixed with a certain amount of PTX in 5 ml of DMSO. The resultant mixture was dialyzed against 1000 ml of deionized water using a dialysis membrane with MWCO of 3500 Da at room temperature. In the first 8 h, the external deionized water was replaced every 2 h, then the external deionized water was replaced every 8 h for 2 days. After dialysis, the solution in the dialysis bag was centrifuged at 3000 rpm for 5 min at room temperature in order to remove unloaded PTX. The supernatant was filtered through 0.8 μm membrane. Then, the drug loaded micelles in supernatant were obtained by freeze drying.

The concentration of PTX loaded DHP–CS–CHO micelles was analyzed by high performance liquid chromatography (HPLC). The HPLC system consisted of a Waters Binary1525 separation module fitted with a waters 2996 photodiode array detector and Dimaohil™ C18 (4.6 mm × 250 mm) column. The mobile phase was the mixture of methanol and water (70:30, v/v) with the elution rate at 0.8 ml/min and the PTX detection wavelength was set at 227 nm. The column was maintained at 25 °C.

PTX release from the PTX loaded micelles was investigated. 2 mg of PTX loaded micelles was dispersed in 2 ml PBS (pH 7.4). The solution was then filled into dialysis bag (MWCO = 3500 Da) and submerged fully into a sealed container with 50 ml PBS containing 0.1% (w/v) Tween 80 with stirring at 100 rpm at 37 °C. At predetermined times, 5 ml external medium was taken outside for HPLC analysis of its PTX content and the same volume of fresh medium was replenished.

2.7. In vitro cytotoxicity assay of paclitaxel loaded micelles

200 μl of MCF-7 cells in RPMI 1640 containing 10% FBS with a cellular density of 1.0×10^4 cells/well was added to each well in a 96-well plate. After incubation for 24 h in incubator (37 °C, 5% CO_2), the culture medium was replaced by 200 μl of RPMI 1640 containing the chitosan derivative and PTX load DHP–CS–CHO micelles with particular concentration, respectively. The cell plate was then returned to the incubator and incubated for 48 h. Then, RPMI 1640 containing polymers were replaced by 180 μl fresh RPMI 1640 and 20 μl of MTT solution (5 mg/ml), followed by

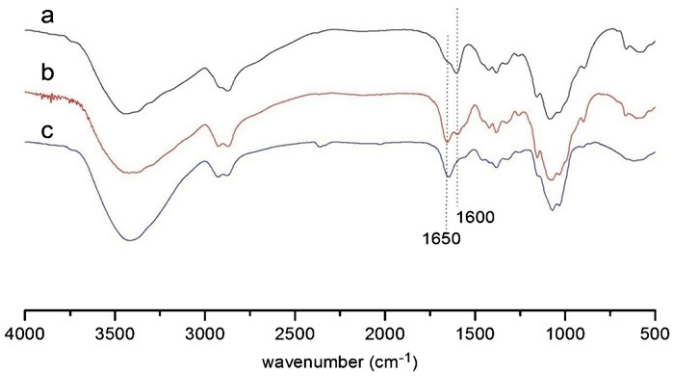

Fig. 2. FTIR of chitosan (a), chitosan–cholic acid (b) and DHP–CS–CHO (c).

incubation for 4 h. After that the culture medium was removed and 200 μl of DMSO was then added and shaken at room temperature. A test wavelength of 550 nm and a reference wavelength of 690 nm were used. The intensity of each well was then given by: (absorbance$_{550\,nm}$ − absorbance$_{690\,nm}$). The relative cell viability was calculated as cell viability (%) = ($OD_{sample}/OD_{control}$) × 100, where $OD_{control}$ was obtained in the absence of polymers, and OD_{sample} was obtained in the presence of polymers. Results were expressed as mean ± SD for five replicates.

3. Results and discussion

3.1. Synthesis of DHP–CS–CHO

Based on amidation reaction which was used frequently in chitosan modification (Jin et al., 2012; Nam et al., 2010; Wang et al., 2011), small hydrophobic molecule cholic acid was grafted on chitosan which was evidenced in the FTIR of chitosan and its derivatives (Fig. 2). The band of amide I at 1650 cm^{-1} (C═O stretch of acetyl group) observably increased while the band of primary amine at 1600 cm^{-1} (N—H bending vibration) decreased, which confirmed the formation of amide linkage between the carboxyl groups of cholic acid and the primary amino groups of chitosan. Amphiphilic chitosan–cholic acid would aggregate together to form micelles in acetic D_2O and cholic acid moiety formed the inner hydrophobic core. The hydrogen affiliated to cholic acid moiety cannot be exchanged freely with D_2O, thus the degree of substitution (DS) of cholic acid could not exactly determined by ^1H NMR. In this study, the DS of cholic acid, which was defined as the number of cholic acid per 100 sugar residues of chitosan, was calculated using the Eq. (1) as follows based on elemental analysis results (C, H and N), the DS of cholic acid in chitosan–cholic acid was 3.0.

$$DS = \frac{(14.00 \times (C/N) - 72.79)}{288.25} \quad (1)$$

As shown in Fig. 2, the peak at 1600 cm^{-1} almost disappeared in DHP–CS–CHO evidenced that small hydrophilic glycidol molecule reacted with primary amine in chitosan–cholic acid via nucleophilic ring-opening reaction under the catalysis of hydrogen ions. The ^1H NMR spectra (Fig. 3) of chitosan and its derivatives further demonstrated the formation of amphiphilic chitosan derivatives, DHP–CS–CHO. The assignments of proton NMR signals were made by comparison with ^1H NMR spectra of chitosan and its derivatives. The broad peak at 2.87–2.98 ppm and peak at 2.50 ppm were attributed to proton of —NH-CH_2— in *N*-(2,3-dihydroxypropyl) moieties. The peak at 2.61–2.79 ppm was from proton at C-2 in saccharide units. The peaks range from 0.66 to 1.90 ppm were ascribed to the protons in cholic acid and also proved the presence of cholic acid moieties in DHP–CS–CHO. The DS of *N*-(2,3-dihydroxypropyl) grafted on chitosan backbone was 50. It was calculated based on the comparison half peak area of —NH-CH_2— in *N*-(2,3-dihydroxypropyl) moieties with that of proton at C-2 in saccharide units.

3.2. Critical micelle concentration (CMC)

The self-aggregation behavior of DHP–CS–CHO and its CMC was determined by pyrene fluorescence probe technique. Fig. 4a showed the increased emission spectra of pyrene in the presence of DHP–CS–CHO with a series of concentrations. It suggested that amphiphilic polymer DHP–CS–CHO supplied pyrene with much more hydrophobic micro-environment when the concentration of polymer increased in PBS. The CMC curves of DHP–CS–CHO determined from emission spectra of pyrene in DHP–CS–CHO aqueous solutions were shown in Fig. 4b. The CMC of DHP–CS–CHO was 0.024 mg/ml in PBS (pH 7.4), which was much lower than that of low molecular weight surfactant, such as SDS with CMC of 2.3 mg/ml. The CMC value also demonstrated that DHP–CS–CHO could form very stable micelles at low concentration in aqueous medium or blood circulation system post administration.

3.3. Size and morphology of DHP–CS–CHO micelles

CMC of DHP–CS–CHO established that this amphiphilic chitosan derivative could self-aggregate in aqueous solution. In the process of DHP–CS–CHO self-aggregated in aqueous medium, several forces influenced the aggregation behavior of amphiphilic chitosan derivative, namely the hydrophobic–hydrophobic associations between cholic acid segments, the hydrogen bonding of hydrophilic segments and water molecules, and the hydrogen bonding among hydrophilic segments. These forces did not only drive the self-aggregation of amphiphilic DHP–CS–CHO polymer but also determined size and morphology of the aggregates. The limpid micellar solution with DHP–CS–CHO at the concentration of 1 mg/ml in PBS was obtained by the sonication. The size and size distribution of the micelles in PBS were determined by dynamic

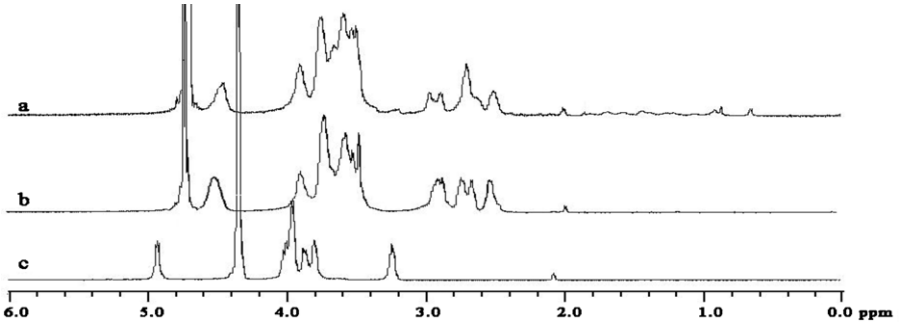

Fig. 3. ^1H NMR spectra of (a) DHP–CS–CHO in D_2O, (b) *N*-(2,3-dihydroxypropyl)–chitosan in D_2O and (c) chitosan in mixture of D_2O/CD_3COOD at 70 °C.

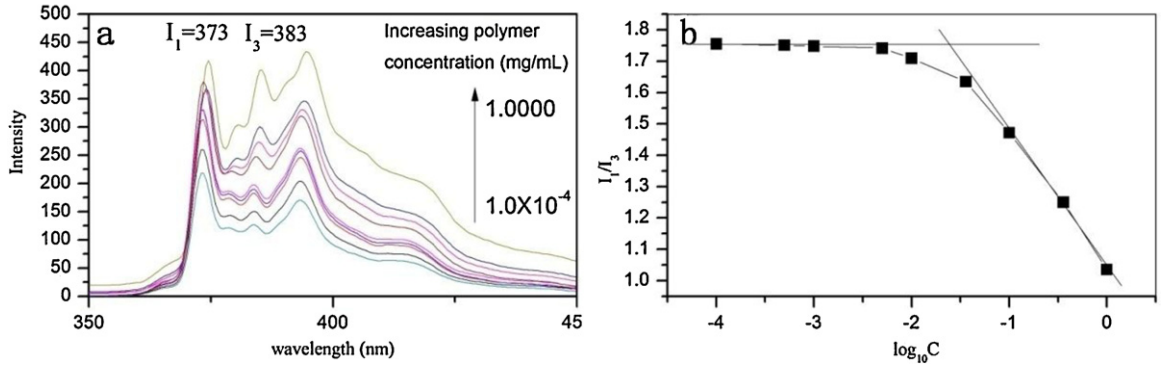

Fig. 4. (a) The fluorescence emission spectra of pyrene against DHP–CS–CHO concentration (excited at 337 nm), (b) plot of the ratio of intensities (I_{373}/I_{383}) from pyrene emission spectra as a function of log *C*.

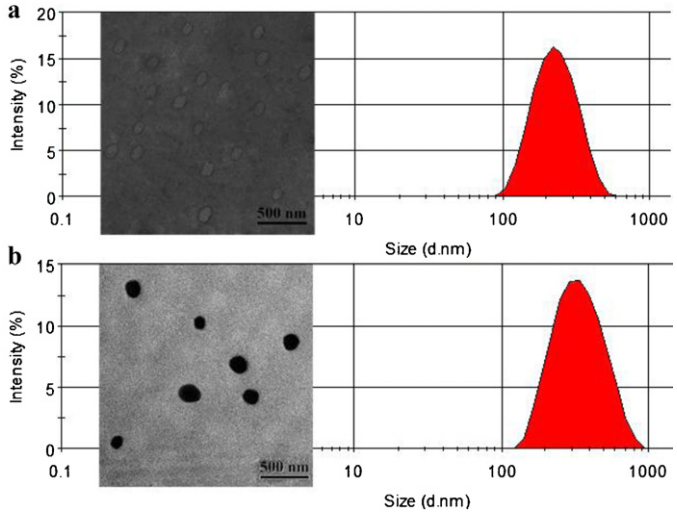

Fig. 5. Size distribution and TEM of DHP–CS–CHO micelles (a) and PTX loaded DHP–CS–CHO micelles (b).

light scattering (DLS). Fig. 5a showed that the size of DHP–CS–CHO micelles was 212.4 ± 3.1 nm with uniform distribution (PDI = 0.147) in PBS. TEM studies also demonstrated that DHP–CS–CHO aggregates were spherical in shape and dispersed well without any aggregation.

3.4. Drug loading and in vitro release

Drug loading and release are important factors investigated in drug delivery system. In the present study, an anticancer drug, PTX was used as model drug to be encapsulated into DHP–CS–CHO micelles by dialysis. Several factors may affect drug loading into the polymeric nanoaggregates and physicochemical properties of polymeric nanoaggregates after drug loading, (1) the affinity of the loaded drug with the core-forming polymer, (2) the content of the hydrophobic core, (3) hydrophobicity of drug, and (4) drug-to-drug interaction (Lee et al., 2010; Zhang et al., 2004). Table 1 showed that drug loading content increased with increase of feed weight ratio of PTX to polymer while loading efficiency increased first, then decreased. This phenomenon may suggest that some PTX molecules have taken part in forming a new hydrophobic core actively and played as a part of segments constructed hydrophobic reservoir for other PTX molecules, therefore the loading efficiency increased first, then decreased when the PTX molecules which formed hydrophobic core actively reached its saturation value. DLS and TEM of PTX loaded DHP–CS–CHO micelles in Fig. 5b demonstrated that the size of micelles (337.8 ± 2.7 nm, PDI = 0.215) increased when PTX was encapsulated into DHP–CS–CHO micelles and the drug loaded micelles changed its structure but still maintained its spherical shape.

PTX is an anticancer drug which has been used in clinic for several years, however, the narrow therapeutic window of PTX and water insoluble physicochemical characteristic limited its application. Therefore, sustained release profile had been proposed in nano-drug delivery system that could reduce the side-effect of PTX. To assess the potential of DHP–CS–CHO micelle as a nano-sized drug carrier, release tests were performed at 37 °C in PBS. Fig. 6a showed that in vitro release profile of PTX from PTX loaded chitosan derivative micelles. PTX keep a sustained release manner from micelles without any burst release nomatter how much PTX was loaded in micelles. It indicated that the release rate of PTX might be controlled by diffusion mechanism as a result of partitioning between micelles and surrounded aqueous phase. In ten days, 40–60% of PTX had been released from PTX loaded micelles with different drug loading content. Fig. 5b showed that when the pH of PBS decreased, the release rate increased because the protonation of primary amine and secondary amine on chitosan backbone chains would increase the repulsive force between inter and intra-chains, then reduced condensity of hydrophobic core. This phenomenon might imply that PTX loaded micelles could easily escape from endosome once entered into cancer cell and release PTX. Among the different PTX loaded chitosan derivative micelles with different loading content of PTX, PTX loaded micelles (loading content = 10.4%) was chosen for further in vitro experiments.

Table 1
Characteristics of PTX loaded DHP–CS–CHO micelles.

Sample	Initial amount of PTX (%)	Loading content of PTX (%)	Loading efficiency (%)
Sample 1	1	0.82 ± 0.07	75.9 ± 7.2
Sample 2	5	4.15 ± 0.60	81.2 ± 5.6
Sample 3	10	8.63 ± 0.71	88.6 ± 7.5
Sample 4	15	10.38 ± 0.67	68.3 ± 6.9

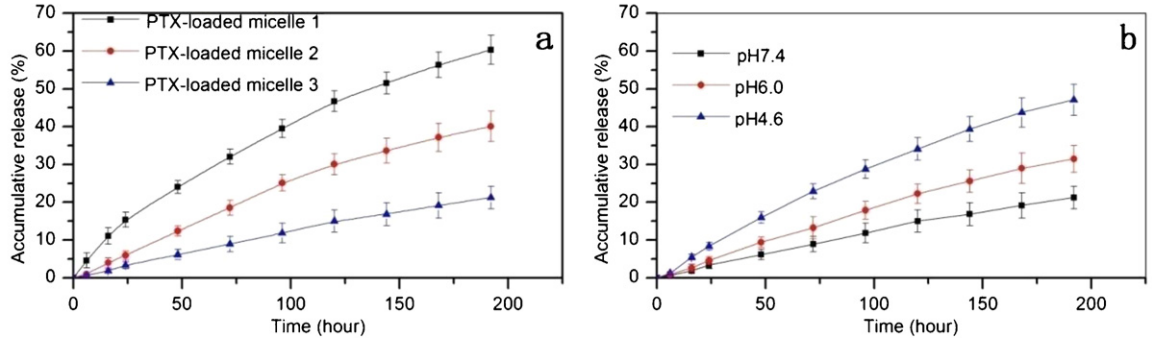

Fig. 6. (a) PTX release profile from PTX loaded amphiphilic chitosan derivatives micelles with different drug loading at 37 °C in PBS (pH 7.4) containing 0.1% Tween 80 (w/v), micelle 1 (loading content = 10.4%), micelle 2 (loading content = 8.6%), micelle 3 (loading content = 4.2%); (b) PTX release profile from PTX loaded micelle 3 at 37 °C in PBS with different pH. Data represent mean ± S.D. (n = 3).

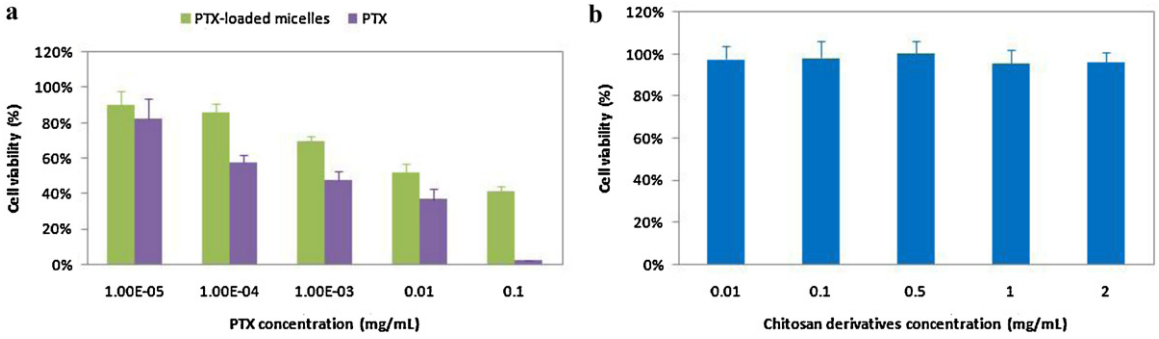

Fig. 7. (a) Cytotoxicity of PTX and PTX-loaded micelles (LD = 10.4%), (b) cytotoxicity of chitosan derivatives, cell viability of each sample was measured using MTT assay, data represent mean ± S.D. (n = 5).

3.5. *In vitro cytotoxicity assay of paclitaxel loaded micelles*

The cytotoxicity of the PTX dissolved in Cremophor EL/ethanol mixture (50/50, v/v) and the PTX-loaded chitosan derivative micelles in PBS was evaluated through an MTT assay. As shown in Fig. 7, the blank chitosan derivative was tested as a control group and almost did not show any cytotoxicity to MCF-7 cells, however, the viability of MCF-7 cells decreased with increase of PTX concentration when the cells cultured with PTX or PTX loaded chitosan derivative micelles for 48 h. PTX dissolved in Cremophor EL/ethanol mixture showed higher cytotoxicity than that of PTX loaded in chitosan derivative micelles. This phenomenon may be ascribed to that PTX loaded in micelles had to be released from micelles before it worked.

4. Conclusion

In the present study, we have synthesized a new kind of amphiphilic chitosan derivative DHP–CS–CHO via simple amidation reaction and nucleophilic ring-opening reaction to prepare micelle for delivery of water-insoluble drug, PTX based on self-assembly. DHP–CS–CHO could form stable spherical micelles (CMC = 0.024 mg/ml) with a narrow and unimodal size distribution in aqueous media even after PTX was loaded in DHP–CS–CHO micelles. The PTX loaded DHP–CS–CHO micelles not only showed sustained release profile of PTX but also displayed significant antitumor activity in vitro while the blank amphiphilic chitosan derivatives micelles demonstrated good biocompatibility. It suggested that DHP–CS–CHO had high potential as a new drug carrier of poorly water soluble anticancer drug, such as PTX.

Acknowledgement

We would like to acknowledge funding from Natural Science Foundation Project of CQ CSTC jja10069 for supporting this work.

References

Chiu, Y. L., Chen, S. C., Su, C. J., Hsiao, C. W., Chen, Y. M., Chen, H. L., et al. (2009). pH-Triggered injectable hydrogels prepared from aqueous N-palmitoyl chitosan: In vitro characteristics and in vivo biocompatibility. *Biomaterials*, *30*, 4877–4888.

Huang, S. T., Du, Y. Z., Yuan, H., Zhang, X. G., Miao, J., Cui, F. D., et al. (2011). Synthesis and anti-hepatitis B virus activity of acyclovir conjugated stearic acid–g-chitosan oligosaccharide micelle. *Carbohydrate Polymers*, *83*, 1715–1722.

Hwang, H. Y., Kim, I. S., Kwon, I. C., & Kim, Y. H. (2008). Tumor targetability and antitumor effect of docetaxel-loaded hydrophobically modified glycol chitosan nanoparticles. *Journal of Controlled Release*, *128*, 23–31.

Jin, Y. H., Hu, H. Y., Qiao, M. X., Zhu, J., Qi, J. W., Hu, C. J., et al. (2012). pH-Sensitive chitosan-derived nanoparticles as doxorubicin carrier for effective anti-tumor activity: Preparation and in vitro evaluation. *Colloids and Surfaces B: Biointerfaces*, *94*, 184–191.

Kalyanasundaram, K., & Thomas, J. K. (1977). Environmental effects on vibronic band intensities in pyrene monomer fluorescence and their application in studies of micellar systems. *Journal of the American Chemical Society*, *99*, 2039–2044.

Kim, K., Kwon, S., Park, J. H., Chung, H., Jeong, S. Y., & Kwon, I. C. (2005). Physicochemical characterizations of self-assembled nanoparticles of glycol chitosan–deoxycholic acid conjugates. *Biomacromolecules*, *6*, 1154–1158.

Kim, T. H., Jiang, H. L., Jere, D., Park, I. K., Cho, M. H., Nah, J. W., et al. (2007). Chemical modification of chitosan as a gene carrier in vitro and in vivo. *Progress in Polymer Science*, *32*, 726–753.

Kumar, M., Muzzarelli, R. A. A., Muzzarelli, C., Sashiwa, H., & Domb, A. J. (2004). Chitosan chemistry and pharmaceutical perspectives. *Chemical Reviews*, *104*, 6017–6084.

Lee, B. S., Park, K., Park, S., Kim, G. C., Kim, H. J., Lee, S., et al. (2010). Tumor targeting efficiency of bare nanoparticles does not mean the efficacy of loaded anticancer drugs: Importance of radionuclide imaging for optimization of highly selective tumor targeting polymeric nanoparticles with or without drug. *Journal of Controlled Release*, *147*, 253–260.

Li, P., Wang, Y., Peng, Z., She, F., & Kong, L. (2011). Development of chitosan nanoparticles as drug delivery systems for 5-fluorouracil and leucovorin blends. *Carbohydrate Polymers*, *85*, 698–704.

Liang, Y., Deng, L., Chen, C., Zhang, J., Zhou, R., Li, X., et al. (2011). Preparation and properties of thermoreversible hydrogels based on methoxy poly(ethylene glycol)–grafted chitosan nanoparticles for drug delivery systems. *Carbohydrate Polymers*, *83*, 1828–1833.

Min, K. H., Park, K., Kim, Y. S., Bae, S. M., Lee, S., Jo, H. G., et al. (2008). Hydrophobically modified glycol chitosan nanoparticles-encapsulated camptothecin enhance the drug stability and tumor targeting in cancer therapy. *Journal of Controlled Release*, *127*, 208–218.

Miwa, A., Ishibe, A., Nakano, M., Yamahira, T., Itai, S., Jinno, S., et al. (1998). Development of novel chitosan derivatives as micellar carriers of taxol. *Pharmaceutical Research*, *15*, 1844–1850.

Muzzarelli, R. A. A. (2009). Chitins and chitosans for the repair of wounded skin, nerve, cartilage and bone. *Carbohydrate Polymers*, *76*, 167–182.

Muzzarelli, R. A. A., Boudrant, J., Meyer, D., Manno, N., DeMarchis, M., & Paoletti, M. G. (2012). Current views on fungal chitin/chitosan, human chitinases, food preservation, glucans, pectins and inulin: A tribute to Henri Braconnot, precursor of the carbohydrate polymers science, on the chitin bicentennial. *Carbohydrate Polymers*, *87*, 995–1012.

Muzzarelli, R. A. A., Greco, F., Busilacchi, A., Sollazzo, V., & Gigante, A. (2012). Chitosan, hyaluronan and chondroitin sulfate in tissue engineering for cartilage regeneration: A review. *Carbohydrate Polymers*, *89*, 723–739.

Nam, T., Park, S., Lee, S. Y., Park, K., Choi, K., Song, I. C., et al. (2010). Tumor targeting chitosan nanoparticles for dual-modality optical/MR cancer imaging. *Bioconjugate Chemistry*, *21*, 578–582.

Ngawhirunpat, T., Wonglertnirant, N., Opanasopit, P., Ruktanonchai, U., Yoksan, R., Wasanasuk, K., et al. (2009). Incorporation methods for cholic acid chitosan–g-mPEG self-assembly micellar system containing camptothecin. *Colloids and Surfaces B: Biointerfaces*, *74*, 253–259.

Oh, N. M., Oh, K. T., Baik, H. J., Lee, B. R., Lee, A. H., Youn, Y. S., et al. (2010). A self-organized 3-diethylaminopropyl-bearing glycol chitosan nanogel for tumor acidic pH targeting: In vitro evaluation. *Colloid and surface B: Biointerfaces*, *78*, 120–126.

Park, J. H., Saravanakumar, G., Kim, K., & Kwon, I. C. (2010). Targeted delivery of low molecular drugs using chitosan and its derivatives. *Advanced Drug Delivery Reviews*, *62*, 28–41.

Trapani, A., Sitterberg, J., Bakowsky, U., & Kissel, T. (2009). The potential of glycol chitosan nanoparticles as carrier for low water soluble drugs. *International Journal of Pharmaceutics*, *375*, 97–106.

Wang, F. H., Chen, Y. X., Zhang, D. R., Zhang, Q., Zheng, D. D., Hao, L. L., et al. (2012). Folate-mediated targeted and intracellular delivery of paclitaxel using a novel deoxycholic acid–O-carboxymethylated chitosan–folic acid micelles. *International Journal of Nanomedicine*, *7*, 325–337.

Wang, F. H., Zhang, D. R., Duan, C. X., Jia, L. J., Feng, F. F., Liu, Y., et al. (2011). Preparation and characterizations of a novel deoxycholic acid–O-carboxymethylated chitosan–folic acid conjugates and self-aggregates. *Carbohydrate Polymers*, *84*, 1192–1200.

Wang, W., McConaghy, A. M., Tetley, L., & Uchegbu, I. F. (2001). Controls on polymer molecular weight may be used to control the size of palmitoyl glycol chitosan polymeric vesicles. *Langmuir*, *17*, 631–636.

Wang, Y. S., Liu, L. R., Weng, J., & Zhang, Q. Q. (2007). Preparation and characterization of self-aggregated nanoparticles of cholesterol–modified O-carboxymethyl chitosan conjugates. *Carbohydrate Polymers*, *69*, 597–606.

Yao, Z., Zhang, C., Ping, Q. N., & Yu, L. L. L. (2007). A series of novel chitosan derivatives: Synthesis, characterization and micellar solubilization of paclitaxel. *Carbohydrate Polymers*, *68*, 781–792.

Yu, J. M., Li, Y. H., Qiu, L. Y., & Jin, Y. (2008). Self-aggregated nanoparticles of cholesterol-modified glycol chitosan conjugate: Preparation, characterization, and preliminary assessment as a new drug delivery carrier. *European Polymer Journal*, *44*, 555–565.

Zhang, C., Ping, Q. N., Zhang, H. J., & Jian, S. (2003). Preparation of N-alkyl–O-sulfate chitosan derivatives and micellar solubilization of taxol. *Carbohydrate Polymers*, *54*, 137–141.

Zhang, C., Qu, G. W., Sun, Y. J., Wu, X. J., Yao, Z. L., Guo, Q. L., et al. (2008). Pharmacokinetics, biodistribution, efficacy and safety of N-octyl–O-sulfate chitosan micelles loaded with paclitaxel. *Biomaterials*, *29*, 1233–1241.

Zhang, L., Hu, Y., Jiang, X., Yang, C., Lu, W., & Yang, Y. H. (2004). Camptothecin derivative loaded poly(caprolactone-co-lactide)-b-PEG-b-poly(caprolactone-co-lactide) nanoparticles and their biodistribution in mice. *Journal of Controlled Release*, *96*, 135–148.

Zheng, H., Zhang, X. Q., Xiong, F. L., Zhu, Z. J., Lu, B., Yin, Y. H., et al. (2011). Preparation, characterization, and tissue distribution in mice of lactosaminated carboxymethyl chitosan nanoparticles. *Carbohydrate Polymers*, *83*, 1139–1145.